State-Level Multidimensional Agricultural Drought Susceptibility and Risk Assessment for Agriculturally Prominent Areas

S M Samiul Islam[1,2]*, Serhan Yeşilköy[1,3], Özlem Baydaroğlu[1], Enes Yıldırım[1], Ibrahim Demir[1,2,4]

[1] IIHR – Hydroscience & Engineering, University of Iowa, Iowa City, Iowa, USA
[2] Civil and Environmental Engineering, University of Iowa, Iowa City, Iowa, USA
[3] Istanbul Provincial Directorate of Agriculture and Forestry, Ministry of Agriculture and Forestry, Istanbul, Türkiye
[4] Electrical and Computer Engineering, University of Iowa, Iowa City, Iowa, USA
[*] Corresponding Author: S M Samiul Islam (smsamiul-islam@uiowa.edu)

Abstract

Due to the shifting climate, extreme events are being observed more frequently globally. Drought is one of the most common natural hazards that severely impacts communities in terms of economic losses and agricultural production disruption. Considering global trade, drought in an agricultural region affects the food security in other regions because of disrupted supply. Decision-makers often consult susceptibility maps when preparing mitigation plans so that the adverse impacts of a drought event can be reduced. Creating drought susceptibility maps can be demanding, requiring a lot of data (i.e., hydrological and land use), expertise, and thorough assessment to accurately picture a vulnerable region's condition. The process also relies on complex hydrological and hydrometeorological models. The objective of this investigation is to examine the vulnerability and impact of drought and formulate maps of drought susceptibility, exposure, and risk by considering a multitude of atmospheric, physical and social indicators. Subsequent to this notion, a fuzzy logic algorithm has been devised by assigning a comprehensive array of weights to each parameter derived from an exhaustive literature review and used for a preliminary investigation for the state of Iowa. This state is located in the Corn Belt region, and its primary economic activity is agriculture. Drought susceptibility maps for the state of Iowa have been generated for the period spanning from 2015 to 2021 and validated using the Kappa coefficient. The produced drought susceptibility maps can support drought mitigation plans and decisions for communities in Iowa.

Keywords: Agricultural Drought Vulnerability, Risk Assessment, Agricultural Susceptibility, Drought Exposure.

1. Introduction

The atmosphere has become warmer, which has caused the intensification of the water cycle (Madakumbura et al., 2019; Tabari, 2020), which is related to extreme atmospheric and hydroclimatological conditions (Seager et al., 2012) such as droughts. Climate change contributes to the increased frequency and severity of droughts and floods worldwide, devastatingly impacting agriculture, ecosystems, city infrastructure (Beck et al., 2010), and human well-being. Rising temperatures and changing precipitation patterns are leading to water scarcity, soil degradation, and increased wildfire risk, exacerbating the negative impacts of the drought (Mukherjee et al., 2018). According to Yuan et al. (2023), drought intensification rates have increased, and the incidence of flash droughts has globally increased by 74% over the past 64 years. Across the world, the number of drought events, affected people, and total damages have increased significantly since the 1990s, rising from 140 to 219 events, 313 to 865 million people, and 73 to $163 billion damage, respectively (EM-DAT, 2023a). The United States has experienced 26 distinct drought episodes, with an estimated total economic loss of 22 billion US dollars (EM-DAT, 2023b). In addition, multi-model ensemble drought projection studies indicate that drought frequency and severity will increase in the future projections globally (Spinoni et al., 2020); regionally (Cos et al., 2022); country level (Islam et al., 2022); and watershed levels in agricultural lands (Yeşilköy and Şaylan, 2022).

Drought is characterized as a multidimensional and insidious hydroclimatological phenomenon due to its gradual occurrence and long-lasting impacts on agriculture (Wang et al., 2014), water resources (Pedro-Monzonís et al., 2015), recreation (Thomas et al., 2013), wildlife (Bodmer et al., 2018), and related communities (Aitkenhead et al., 2021). Agricultural drought is characterized by a shortage of soil moisture (SM) resulting from a lack of precipitation over a specific period (Sepulcre-Canto et al., 2012). When SM declines below the wilting point of the soil, crop yield is adversely impacted, resulting in reduced production of crops (Lobell et al., 2011). The costs and losses associated with agricultural drought-related output are increasing dramatically (García-León et al., 2021), making it challenging to quantify precisely in terms of spatial extent and intensity. The success of drought preparedness and mitigation depends on timely information on drought onset, progress, and extent obtained through effective drought monitoring. Effective monitoring of water resources requires extensive effort on instrumentation via sensor networks, remote sensing and citizen science efforts (Demir et al., 2015). Typically, drought monitoring involves using drought indicators like the Standardized Evapotranspiration and Precipitation Index (SPEI; Vicente-Serrano et al., 2010) and the Evaporative Demand Drought Index (EDDI; Hobbins et al., 2016) at different time scales (Tian et al., 2018), which can provide estimates of the severity of drought and track its propagation (Schumacher et al., 2022).

Droughts can cause significant economic losses, particularly in agricultural regions where crops and livestock are vulnerable to water shortages (O’Neill et al., 2020). It is a severe natural hazard that affects many regions of the world, including the Midwestern region of the US (Mallya et al., 2013), where it poses a significant threat to agricultural production (Dai, 2011). The US Midwest (or corn belt) is prone to droughts, with Iowa being one of the most agriculture-dominant states that can be severely affected. Drought conditions in Iowa can lead to crop failures, water scarcity, and economic losses (Hatfield and Prueger, 2015). In 2021, more than half of the Iowa counties were declared beneficiaries of the Emergency Relief Program due to droughts (USDA, 2021a). Climate change is increasing the frequency and intensity of droughts in the corn belt (Zhou et al., 2021), making it crucial to develop effective drought assessment and management tools. In recent years, there has been growing concern about the impact of climate change on the frequency and intensity of droughts in the Midwest. Studies have shown that climate change is likely to increase the risk of droughts in the region, making it imperative to develop effective drought assessment and management tools (Walthall et al., 2012). The literature emphasizes the significance of addressing Iowa's susceptibility to agricultural droughts.

In January 2023, the Iowa Drought Plan was developed to work on an approach to address the increasing frequency and intensity of droughts in the state, and prepare for, identify, respond to and recover from the drought events. The plan consists of several strategies to improve water management, reduce water demand, and enhance water conservation. Along with the real-time monitoring effort, the plan utilized National Risk Index products such as the Drought Risk Index and Expected Annual Losses (Iowa DNR, 2023). Although these resources are valuable for assessing drought vulnerability, their resolutions are inadequate to provide detailed information on the state of the drought. High-resolution drought maps are crucial for effective drought management and mitigation. These maps can provide detailed information about the extent and severity of drought conditions, which can help decision-makers and stakeholders identify vulnerable areas and prioritize resources for drought response. High-resolution drought maps can also aid in developing early warning systems and improve the accuracy of drought forecasting. In addition, these maps can assist in assessing drought impacts on various sectors, including agriculture, water resources, and public health.

With the rapid development of geospatial technologies, such as remote sensing and Geographic Information System (GIS) technology, they have become increasingly popular for monitoring (Sermet and Demir, 2023) water hazards (i.e., drought and flooding) and environmental analysis (Xu et al., 2019), due to their microscopic view, affordability, comprehensive coverage, and high spatial and temporal resolution. Web based libraries and systems provide significant potential in communicating (Demir et al., 2009) and analyzing geospatial data (Sit et al., 2019) to support informed decisions. A recent review of agricultural drought indices derived from remote sensing has demonstrated significant research progress and classification, including SM and crop water demand indices (Kumar et al., 2013; Mani and Varghese, 2018). Remote sensing, in particular, has been extensively used to monitor flooding (Li and Demir, 2023), vegetation health, soil moisture, and air temperature, critical indicators of drought conditions (Wang et al., 2019). These datasets can be obtained from various sources, including satellites, aircraft, and ground-based sensors (Muste et al., 2017), and can provide valuable information on the spatial and temporal variability of drought conditions. In addition, monitoring crop water demand conditions derived from remote sensing is generally reflected through crop morphological, physiological, and comprehensive indices (Yang and Wu, 2010).

Fuzzy logic-based approaches are another essential risk analysis and assessment technique that has gained popularity in recent years. In the field of natural hazard mapping, previous studies have utilized multiple criteria decision methods (MCDM), such as the analytic hierarchy process (AHP), the fuzzy analytic hierarchy process (FAHP) approach (Cikmaz et al., 2023), fuzzy logic (Hoque et al., 2021), data analytics (Alabbad et al., 2022), statistical models, and machine learning (Sit et al., 2021). For instance, Hoque et al. (2021) used a heuristic approach by integrating fuzzy logic to map agricultural drought vulnerability. These models are recognized as being among the essential hazard assessment tools. However, multicriteria decision-making is considered more accurate and less subjective when using fuzzy logic, reducing imprecision and subjectivity (Zhao and Li, 2016). This fuzzy logic-based method is artificial intelligence that can handle uncertain and imprecise data. They are beneficial for drought assessment because drought conditions are often complex and challenging to define, and uncertainty is often associated with the data used to assess drought conditions. Fuzzy logic-based methods can help overcome these challenges by providing a more flexible and adaptable approach to drought assessment (Nikolova et al., 2021).

There are various efforts in the literature to assess agricultural drought vulnerability. Ekrami et al. (2023) used the AHP approach for arid and semiarid regions and validated agricultural drought vulnerability maps with specific ground control points (GCP). Senapati et al. (2021) employed AHP and weighted overlay techniques for West Bengal. Block-wise productivity data was used in this study, and a visual cross-correlation study was employed for validation. Mokarram et al. (2021) used the MCDM coupled with a cellular automaton (CA)-Markov model for Iran, using the receiver operating characteristic (ROC) curve for validation.

Wu et al. (2017a) evaluated global vulnerability to agricultural drought. They created the agricultural drought vulnerability index, composed of the weight of the seasonal crop water deficiency ratio, the importance of the soil’s available water-holding capacity, and the weight of the irrigated area proportion. They chose global agricultural cultivation regions as the study area and identified six main crops as the hazards-affected body of agricultural drought. Another drought vulnerability index for Zacatecas was developed by Ortega-Gaucin et al. (2021) based on a collection of socioeconomic and environmental parameters and utilizing sensitivity and adaptive capacity indices. To assess the agricultural drought susceptibility of Yunnan Province in China, Wu et al. (2017b) developed a comprehensive approach based on a vulnerability scoping diagram (VSD) model that emphasizes the human-land link by considering both natural circumstances and human activities. Zarei et al. (2021) used AHP to assess the susceptibility of several forms of drought in Iran, including meteorological, hydrological, and agricultural droughts. A consistency index was employed for the validation of the results.

Some researchers have validated their findings using a consistency index (rate). For instance, Kundu et al. (2021) used AHP to estimate drought vulnerability in India from a socioeconomic perspective. Wijitkosum and Sriburi (2019) used the fuzzy AHP (FAHP) to examine desertification risks for Thailand by concentrating on climatic, physical, soil, and land use aspects. In this study, a consistency test was performed. Zarei and Mahmoudi (2022) used FAHP and the second-order Markov Chain to predict agricultural drought vulnerability in Iran, and they applied a compatibility ratio to estimate the accuracy of the results. Sivakumar et al. (2021) employed MCDM and AHP for India. Stephan et al. (2023) applied two weighting methods with multicriteria inputs in the pre-Alpine region. The validation process was conducted via interviews with stakeholders. Utilizing an entropy-fuzzy pattern recognition-based model, Zhou et al. (2022) identified the key contributors to a city's drought susceptibility: precipitation, water usage effectiveness, and irrigation protection area rate. Moreover, the severity of agricultural drought susceptibility in China was assessed by Guo et al. (2021) using the weighted comprehensive score approach and the entropy weight method.

These models are essential hazard assessment tools (Hoque et al., 2021; Nikolova et al., 2021). However, when using fuzzy logic, multicriteria decision-making is considered more accurate (Chen et al., 2020) and less subjective (Mahjouri et al., 2017), as it reduces imprecision and subjectivity (Kahraman, 2008). This fuzzy logic-based method resembles human reasoning to handle uncertain and imprecise data. They are beneficial for drought assessment (Pesti et al., 1996) because drought conditions are often complex and challenging to define due to their chaotic nature (Baydaroğlu Yeşilköy et al., 2020). Fuzzy logic-based methods can help to overcome these challenges by providing a more flexible and adaptable approach to drought assessment. We will use remote sensing (soil moisture) and meteorological (air temperature, precipitation) data to develop a fuzzy logic-based drought index incorporating multiple variables, vegetation health, etc.

Considering that Iowa is one of the most vulnerable states and is an agricultural production stronghold, understanding hazard susceptibility is critical to inform decision-makers about taking the necessary actions to minimize losses (Yildirim and Demir, 2022). Additionally, the state's essential role in food production requires examining the phenomenon. Also, fuzzy-based artificial intelligence has not been adopted to investigate drought conditions statewide, which can generate insights into the state's vulnerability to natural disasters. To close the gap, this research aimed to (1) develop a fuzzy logic-based geospatial technique for agricultural drought assessment in Iowa; (2) create an agricultural drought vulnerability map for the corn and soybean farming systems based on multicriteria analysis; (3) analyze the spatiotemporal variability of drought conditions in the state and identify the most vulnerable regions to drought; and (4) provide potential agricultural drought event mitigation and adaptation strategies for stakeholders like decision-makers, agriculturists, and farmers. To achieve these objectives, we carried out an extensive literature review on drought assessment, geospatial techniques and fuzzy logic-based approaches for the analysis.

The manuscript was structured as follows: In the methods section, we describe data sources and methodology, including selecting variables and developing the fuzzy logic-based index. In the results section, we present the results of our analysis, including the validation of the index using ground-based data and the spatiotemporal variability of drought conditions in Iowa. We then discuss the implications of our findings for drought management and adaptation strategies. In conclusion, we conclude the paper and provide recommendations for future research.

2. Materials and Methods

2.1. Study Area

The state of Iowa is located in the U.S. Midwest or Corn Belt (Latitude: 40° 23′ N to 43° 30′ N and longitude: 90° 8′ W to 96° 38′ W) with an area of 145,746 km². It is bordered by six other states: Illinois to the east, Minnesota to the north, Nebraska to the west, Wisconsin to the northeast, Missouri to the south, and South Dakota to the northwest. According to the Köppen-Geiger climate classification (Beck et al., 2018), Iowa has a humid continental climate. Average temperatures in July, the hottest month, range from 22°C in the north to 27°C in the south, while average temperatures in January, the coldest month, range from -12°C in the north to -5°C in the south. The state receives a mean annual total precipitation of 858 mm, with the heaviest rainfall in May and June.

Agriculture is the backbone of Iowa's economy, with approximately 85% of its land area dedicated to farmland (Iowa Farm Facts, 2023). The state is a leading producer of corn, soybeans, pork, and eggs, among other commodities (USDA, 2021). The topography of Iowa is relatively flat, with an elevation ranging from 146 m above sea level in the southeastern part of the state to 509 m in the northwestern region. The state is drained by several major river systems, including the Missouri River, which forms the state's western border, and the Mississippi River, which includes the eastern border. The state also has numerous smaller rivers, streams, and lakes as seen in Figure 1.

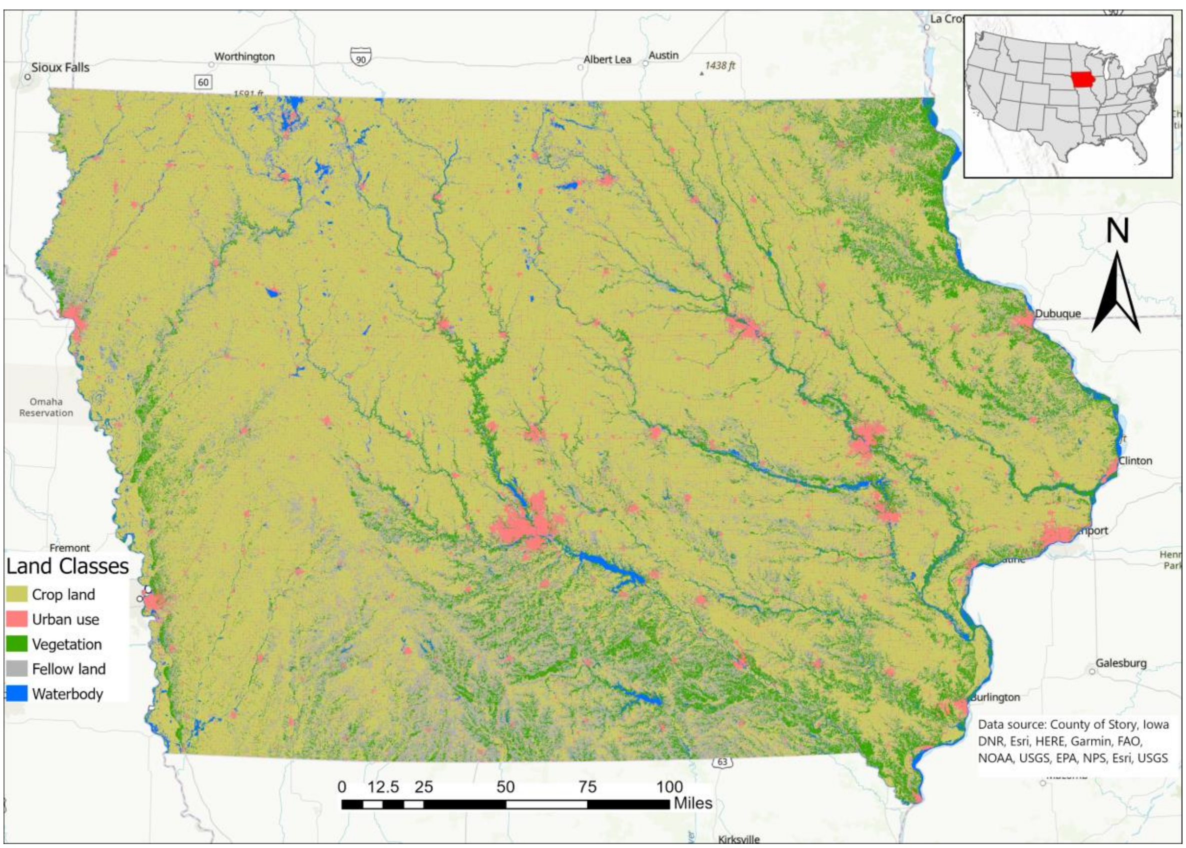

Figure 1. Land classes and location of the study area, State of Iowa.

Despite its relatively high average annual precipitation, Iowa is still vulnerable to drought in recent years (Leeper et al., 2022). Droughts in the state can lead to crop failures, water scarcity, and economic losses. In recent years, several severe droughts in Iowa, including in 2012 and 2021, significantly damaged crops and livestock (NOAA, 2023). The Midwest area is predicted to experience more frequent and severe droughts due to climate change, necessitating the creation of practical drought assessment and management techniques.

The state is split into nine crop reporting districts for agricultural purposes, and the US Department of Agriculture (USDA) uses these districts to record crop yields and output (USDA, 2021b). These districts are based on soil type, climate, and agricultural practices and provide a useful framework for analyzing agricultural drought at a regional level. The major crops grown in Iowa are corn and soybeans, which account for approximately 90% of the state's crop acreage (USDA, 2021). Livestock production is also an important sector of Iowa's agricultural industry, with the state ranking first in the nation in the production of pork and eggs. The study area, Iowa, is the 26^{th} largest state in the US and one of the leading agricultural states in the country. The study period covered 2015 to 2021, which provided a 7-year time frame for the analysis. Overall, Iowa's unique geographic and climatic characteristics and strong agricultural sector make it an important region to study in the context of agricultural drought assessment and management.

2.2. Data

The data used in this research came from various sources (Table 1). The National Oceanic and Atmospheric Administration (NOAA) and the National Centers for Environmental Information (NCEI) provided the climatic data, which included precipitation and temperature (NOAA, 2021). The soil moisture data were obtained from the North American Land Data Assimilation System (NLDAS) (Beaudoing et al., 2021). The crop yield data were obtained from the U.S. Department of Agriculture's (USDA) National Agricultural Statistics Service (NASS) (USDA, 2021b). The land use data were obtained from the USDA National Agricultural Statistics Service (NASS) Cropland Data Layer (CDL) (USDA, 2021c). Slope (percentage rise) was calculated using the Digital Elevation Model (DEM) data at 30 m spatial resolution.

Table 1. Data and its type, spatial resolution, and source are listed.

Indicator	**Data Type**	**Spatial Resolution**	**Data Source**	**Time Period**
Land Use Land Cover (LULC)	Raster data	10 m	Iowa DNR https://programs.iowadnr.gov/geospatial/rest/services/LandCover/LC_2009_1m/MapServer	2019
Soil type	Shapefile	N/A	USDA website https://www.nrcs.usda.gov/conservation-basics/natural-resource-concerns/soil	2021

Soil moisture content (Percentile)	Raster data	0.125°	Beaudoing et al. (2021) https://doi.org/10.5067/UH653SEZR9VQ	2015-2021
Digital elevation model (m)	Raster data	30 m	Earth explorer (SRTM DEM) https://earthexplorer.usgs.gov/	2019
Daily total precipitation (mm)	Raster data	4 km	gridMET: https://www.climatologylab.org/gridmet.html	2015-2021
Daily maximum air temperature (°C)	Raster data	4 km	gridMET: https://www.climatologylab.org/gridmet.html	2015-2021
Daily total potential evapotranspiration (mm)	Raster data	4 km	gridMET: https://www.climatologylab.org/gridmet.html	2015-2021
Distance from waterbody (m)		30 m	Geo data of Iowa https://geodata.iowa.gov/search?collection=Document	2021
Distance from road (m)	Shapefile	30 m	The TIGER/Line shapefiles and related database files of the U.S. census https://catalog.data.gov/dataset/tiger-line-shapefile-2015-state-iowa-primary-and-secondary-roads-state-based-shapefile	2021
Population density (people/km^2)	Shapefile	N/A	ACS 2021 (2017-21, 5-year estimation) from National Historical Geographic Information System (NHGIS) https://www.nhgis.org/	2021

2.2.1. Indicators of Agricultural Drought Vulnerability Mapping

Agricultural drought is often associated with four parameters: soil type, precipitation, soil moisture, air temperature, and potential evapotranspiration (PET; Narasimhan and Srinivasan, 2005). This study considered all these parameters for the study period (Dayal et al., 2017). The growth of crops largely depends on the soil's moisture content. In addition, the type of soil also plays an essential role in ensuring nutrients and water for growth (Jain et al., 2015). Soil containing a higher proportion of loam and clay has a greater capacity to retain water than sandy soil. Consequently, regions with higher levels of sand content in their soil are at an increased risk of experiencing drought. The soil type data was obtained from the US Department of Agriculture, Natural Resources Conservation Service (USDA, 2016), and daily SM data from NASA-GRACE (Beaudoing et al., 2021).

Various climatic variables, such as maximum air temperature (T_{max}), evapotranspiration (ET), and precipitation (P), have a significant impact on the susceptibility of regions to agricultural drought (Dahal et al., 2016). These variables strongly associate with agricultural productivity and play a critical role in determining the level of exposure to drought conditions in each region. Precipitation is one of the most essential variables influencing agricultural drought. Low precipitation levels intensify drought conditions, adversely affecting agricultural productivity. Consequently, regions with low levels of rainfall are generally more susceptible to agricultural drought than regions with high levels of rainfall. In contrast, areas with low temperatures and evapotranspiration are less vulnerable to the effects of agricultural drought. These climatic variables tend to have a mitigating effect on drought conditions, reducing the overall susceptibility of an area to drought.

The approach employed in data analysis followed a series of distinct phases. Firstly, the NetCDF format data was converted to raster format. Subsequently, the average of all year data was calculated through ArcGIS' raster calculator, and this information was integrated into a single raster layer. The soil type data for 2016 was obtained as a shape file from the USDA, and it was classified based on its relevance to agricultural drought susceptibility. This thorough process ensured that a comprehensive data analysis was conducted, and the results were grounded in robust and reliable data.

2.2.2. Indicators of Exposure Mapping

The concept of exposure within the context of hazard assessment refers to the elements of a given area that are susceptible to the impact of a potential disaster. These elements include the population, infrastructure, and built surfaces that may be vulnerable to damage in the event of a hazard. Various indicators are utilized to effectively map the level of exposure within a given region, such as land use and land classification (LULC), as well as population density (Wu et al., 2017c). In the specific case of the state of Iowa, the LULC data reveals that the majority of the land is utilized for various types of crop cultivation. However, when considering the weight of each classification in terms of their susceptibility to hazard exposure, barren or fallow lands are deemed the most vulnerable. This contrasts with water bodies, vegetation, and snow cover, considered the least exposed to regional hazards. A nuanced understanding of the level of exposure within a region is vital to implementing effective disaster risk reduction strategies and ensuring the safety of those who reside within the area.

The population data were collected from the National Historical Geographic Information System (NHGIS) following the 2021 census (Steven Manson, 2021). It has been widely recognized that population density can have a significant impact on the occurrence of food scarcity and famine in a given region. In areas with high population density, the demand for resources such as food and water can often exceed the available supply, leading to scarcity becoming a genuine concern. This can be exacerbated by severe drought conditions, which can further limit the available resources and make it increasingly difficult for people to access the necessary food and water. The effects of famine can be particularly devastating, as they can lead to serious health issues and even the loss of life in some cases. Moreover, they can have significant social and economic consequences, compounding the negative impact on affected communities. Therefore, it is essential to develop effective strategies for mitigating the effects of food scarcity and famine, especially in regions with high population density. Figure 2 (a-e) shows land use and land cover, distance to roads, distance to water bodies, soil type, elevation, and population density maps.

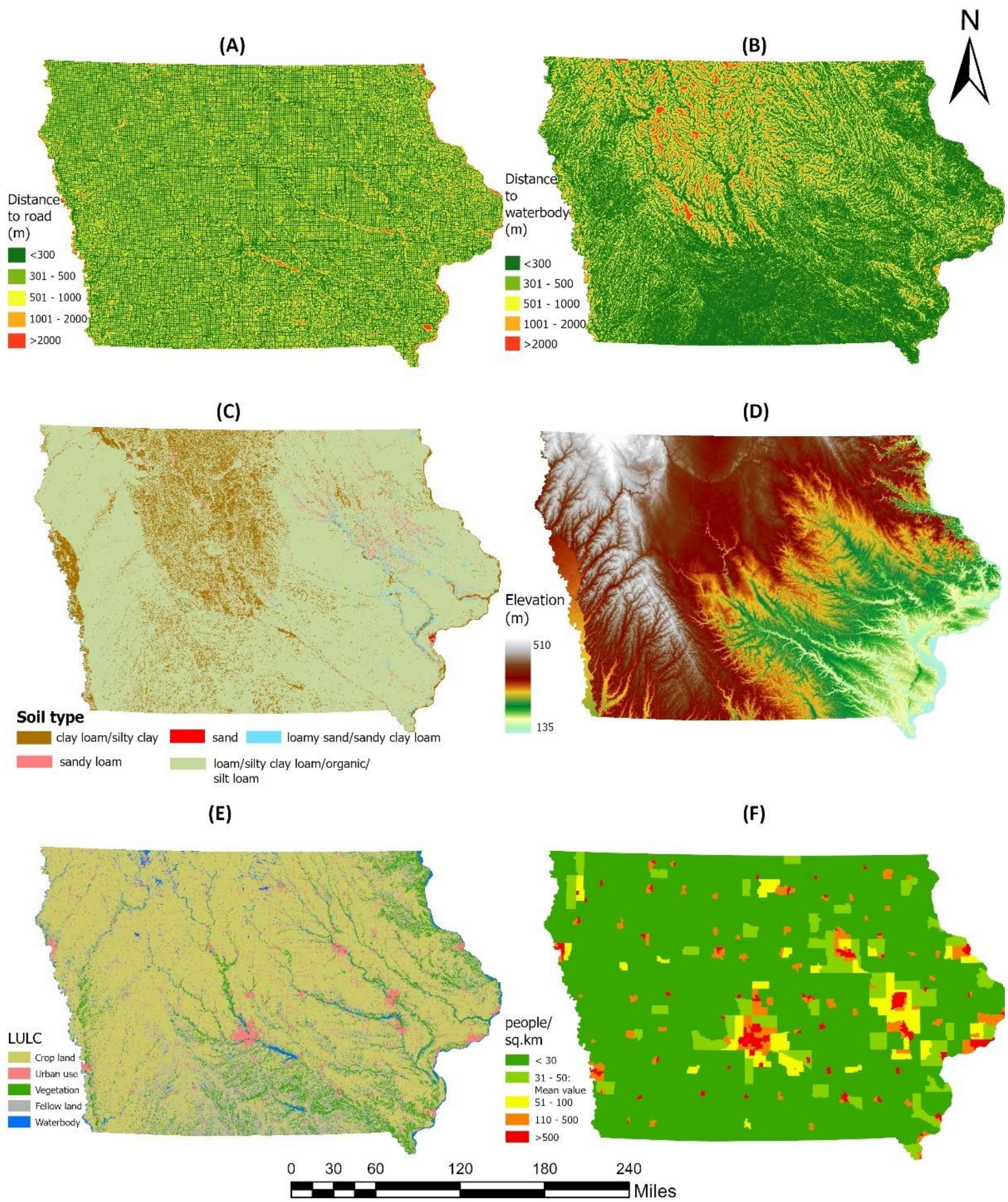

Figure 2. (a) Distance to road map (b) Distance to waterbody (c) Soil type (d) Elevation (e) land use and land class, and (f) Population density (people/sq.km) map.

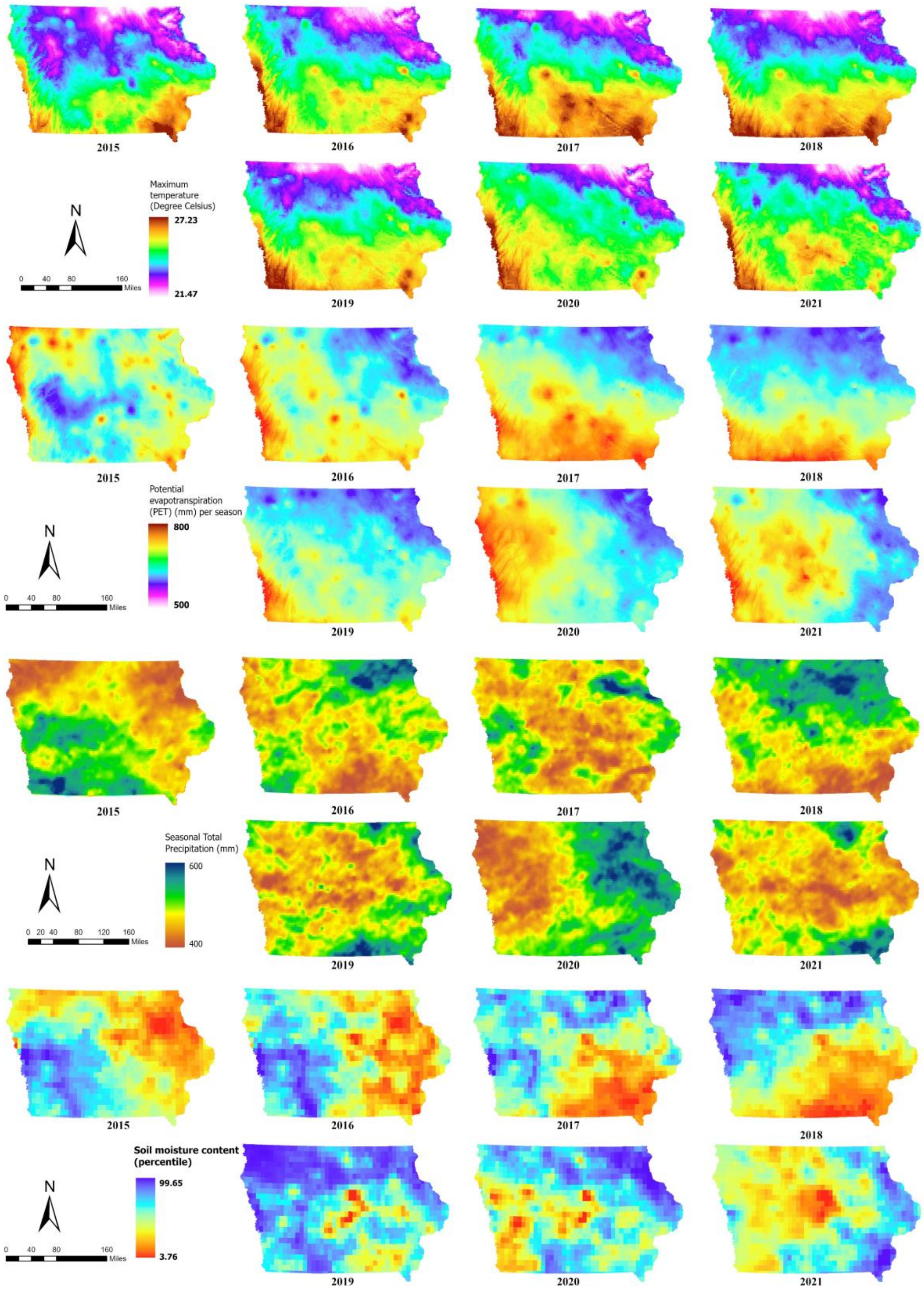

Figure 3. (a) Maximum air temperature (b) Total PET (c) Total Precipitation (d) Soil moisture maps of Iowa between the 2015 and 2021 years.

T_{max}, PET, precipitation, soil water content, and fuzzy vulnerability maps during the agricultural production between 2015 and 2021 can be found in Figures 3 (a-d). Looking at the T_{max} maps, it can be seen that Iowa's middle, west, southwest, and southeast regions are exposed to higher temperatures, almost like a semicircle. In contrast, lower temperatures are observed at relatively high latitudes in the study area (Fig. 3 (a)). The observed gradual decline in the maximum temperature distribution from the southern to the northern regions, as depicted in Fig. 3 (a), can be attributed to the latitudinal effect resulting in a decrease in temperature. The observed decline in areas with lower maximum temperatures between 2015 and 2021 is noteworthy.

Since PET values are calculated from atmospheric variables such as air temperature, wind speed, and relative humidity, they have similarities with the temperature map. Therefore, its spatial and temporal resolution can be considerably varied. As seen in Figure 3 (b), the spatial variation of PET values is high. The spatiotemporal variability of precipitation levels ranging from 400 to 600 mm during the agricultural production period in Iowa is significant (Fig. 3 (c)). The variability of PET values within the range of 500–800 mm suggests that the soil water budget may exhibit susceptibility to drought conditions. Furthermore, the occurrence of snow droughts during the winter months has the potential to exacerbate agricultural drought conditions during the summer season (Yeşilköy et al., 2023).

When reviewing the soil water content maps (Fig. 3 (d)) generated for Iowa, it is evident that regions with low soil water content coincide with areas experiencing low precipitation amounts and high PET values during the summer. In the 2021 map of SM, the central Iowa region is characterized by a significant deficit in SM. It can be said that the precipitation levels during this episode are relatively insufficient, measuring approximately 400 mm, while the PET values are in the range of 750-800 mm. Considering that the PET-P amounts range between 350-400 mm, it is thought that such values could potentially result in agricultural drought. Based on the presented maps, it can be clearly stated that the occurrence of meteorological drought does not necessarily imply the presence of agricultural drought in the corresponding regions.

2.3. Fuzzy Membership Functions and Weight Assignments

The assignment of weights is an essential component of various types of research, including risk assessment, vulnerability mapping, and decision-making. To accomplish this task comprehensively and effectively, fuzzy membership functions can express uncertainty and vagueness (Pramanik et al., 2020). Fuzzy membership functions help quantify an element's membership degree to a particular class or category, with values from 0 to 1, where 1 signifies full membership and 0 represents no membership. By utilizing fuzzy membership functions, subjectivity and uncertainty can be incorporated into the weight assignment process, producing more accurate and dependable outcomes. This approach has been successfully applied in various disciplines, such as environmental management, urban planning, and decision-making under conditions of uncertainty. As such, the application of fuzzy membership functions in weight assignment has emerged as a valuable tool for researchers seeking to improve the accuracy and reliability of their analyses.

Applying fuzzy membership functions in drought assessment is a vital step involving several stages. The initial phase consists of classifying drought indicators into distinct classes using various methods such as manual classification, equal intervals, and natural breaks. The classified indicators are then reclassified and assigned numbers from 0 to 5 based on their contribution to agricultural drought in the ArcGIS environment. Fuzzy membership functions such as fuzzy-large, fuzzy-small, and linear are then assigned to the reclassified dataset based on their direct or inverse relationship with agricultural drought vulnerability. Some factors such as soil type, elevation, T_{max}, PET, and distance to water bodies, which directly relate to vulnerability, are assigned fuzzy-large functions.

In contrast, indicators like soil moisture and total rainfall, which have an inverse relationship with vulnerability, are assigned fuzzy-small functions. Additionally, the population density has a linear relationship with vulnerability and, thus, is assigned a fuzzy-linear function. The procedures used in the study, including fuzzy-large and fuzzy-small, are presented in equations (1) and (2), respectively. The rationale for using these functions and their characteristics is further explained by Mullick et al. (2019).

$$\mu_1\,(x) = \frac{1}{1 + (\frac{x}{f2})^{-f1}} \tag{1}$$

$$\mu_2\,(x) = \frac{1}{1 + (\frac{x}{f2})^{\,f1}} \tag{2}$$

where, both the spread (f1) and the data midpoint values were specified by the default functions of the membership functions as the functions set the value quantifying the data distribution. Here, x is the value of the input raster file and "μ_1" and "μ_2" are the Fuzzy-large and Fuzzy-small functions, respectively. Table 2 shows the drought indicators used in the study, their assigned weights, and susceptibility levels with fuzzy membership functions.

Table 2. Assigned weight and fuzzy membership function against the agricultural drought indicators.

Drought Indicators	**Class Break Value**	**Susceptibility Level**	**Weight**	**Membership Function**	**Notes / Assumptions**
LULC	Crop land	Very high	1	Fuzzy-small	Inversely related to agricultural drought
	Urban/Built-up	High	2		
	Vegetation	Moderate	3		
	Grassland	Low	4		
	Barren / Fellow land	Very low	5		
	Water	Non-member	-10		
Soil type	Sandy	Very high	5	Fuzzy-small	
	Sandy loam/rocky	High	4		

	loamy sand/sandy clay loam	Moderate	3		Inversely related to agricultural drought
	loam/silty clay loam/organic/silt loam	Low	2		
	clay loam/silty clay/clay	Very low	1		
Soil moisture content (Percentile)	< 24.65	Very high	5	Fuzzy-small	Inversely related to agricultural drought
	24.66 – 38.25	High	4		
	38.26 – 48.83	Moderate	3		
	48.83 – 67.37	Low	2		
	< 67.38	Very low	1		
Digital Elevation Model (m)	< 245	Very low	1	Fuzzy-large	Directly related to agricultural drought and has a direct association with that.
	245 – 298	Low	2		
	298 – 345	Moderate	3		
	345 – 393	High	4		
	>= 393	Very high	5		
Slope (percentage rise)	0 – 2	Very low	1	Fuzzy-large	Directly related to agricultural drought and has a direct association with that.
	2 – 4	Low	2		
	4 – 6	Moderate	3		
	6 – 8	High	4		
	>8	Very high	5		
Seasonal total precipitation (mm)	< 410.62	Very high	5	Fuzzy-small	Inversely related to agricultural drought
	410.62 – 494.77	High	4		
	494.77 – 508.97	Moderate	3		
	508.97 – 578.94	Low	2		
	> 578.94	Very low	1		
Seasonal mean T_{max} (°C)	< 23.25	Very low	1	Fuzzy-large	Directly related to agricultural drought and has a direct association with that.
	23.25 – 23.87	Low	2		
	23.87 – 24.55	Moderate	3		
	24.55 – 25.26	High	4		
	> 25.26	Very high	5		
Seasonal total PET (mm)	< 523.44	Very low	1	Fuzzy-large	Directly related to agricultural drought
	523.44 – 530.34	Low	2		
	530.34 – 638.27	Moderate	3		
	638.27 – 646.84	High	4		
	> 646.84	Very high	5		
Distance from	< 300	Very low	1	Fuzzy-large	
	300 – 500	Low	2		

waterbody (m)	500 – 1000	Moderate	3		Directly related to agricultural drought
	1000 – 2000	High	4		
	> 2000	Very high	5		
Distance from road (m)	< 300	Very low	1	Fuzzy-large	Directly related to agricultural drought
	300 – 500	Low	2		
	500 – 1000	Moderate	3		
	1000 – 2000	High	4		
	> 2000	Very high	5		
Population density (people / km^2)	< 1	Very low	1	Fuzzy-linear	Directly related to agricultural drought
	1 – 5	Low	2		
	5 – 10	Moderate	3		
	10 – 20	High	4		
	> 2500	Very high	5		

2.4. Assessment of Vulnerability, Exposure and Drought Risk

Following the assignment of weights to the indicators using fuzzy-membership functions, the indicators were normalized to a 0-1 scale, where 0 denotes a low association with drought, and 1 denotes a high association. Subsequently, the fuzzy overlay function in the ArcGIS toolbox was employed to quantify vulnerability and exposure. The fuzzy overlay function offers five operators: SUM, AND, OR, PRODUCT, and GAMMA. The GAMMA overlay operation was utilized in the current study due to its effectiveness in agricultural drought assessment, as indicated by Dayal et al. (2017) and Hoque et al. (2021). Once the vulnerability map was generated, the exposure indicators were multiplied with the vulnerability map to quantify exposure due to vulnerability.

The process of assessing the risks of an agricultural drought entails identifying and mapping the physical and socioeconomic elements that influence its incidence and severity. Vulnerability indicators are physical or environmental elements that influence the likelihood and severity of drought, such as SM content, rainfall, max air temperature, and evapotranspiration rates. Socioeconomic variables that determine how well populations or systems can adapt to the effects of drought include soil type, land use and cover, and population density. ArcGIS's fuzzy overlay Gamma function (Eq. 3) combined hazard and vulnerability indicators to create a composite risk map that displays regions with high and low agricultural drought risk. The generated map can assist decision-makers in prioritizing locations for focused intervention and identifying regions needing mitigation measures to lower the risk of agricultural drought. The equation for the gamma distribution function is below:

$$f(x) = \begin{cases} \frac{x^{p-1}e^{-x}}{\Gamma_{\mathrm{p}}} \; p > 0, 0 \leq x < \infty \\ 0 \; otherwise \end{cases} \tag{3}$$

where p and x are continuous random variables. The gamma function is Γ(y), a complex number version of the factorial function. So, the Equation 4 for the agricultural drought risk map was used.

$$Drought\ risk\ map = Drought\ vulnerability\ x\ Exposure\ of\ drought \qquad (4)$$

3. Results and Discussion

Multiple drought risk maps were produced based on the data and approach, the drought vulnerability, exposure, and finally, using the vulnerability and exposure data. We provide more details on our findings in the following sections.

3.1. Fuzzy Vulnerability of Drought Indicators

The fuzzy vulnerability of the different indicators is shown in Figure 4 (a-f). Due to numerous circumstances, most of the region is classified as having a very low or low level of agricultural vulnerability. Inadequate infrastructure, such as limited road connectivity, impedes the transport of agricultural inputs and outputs, making it difficult for producers to engage in efficient agricultural practices. In addition, limited access to dependable water sources and insufficient irrigation systems limits agricultural productivity, forcing farmers to rely on rain-fed agriculture or limiting specific crop cultivation. As Iowa has good road network facilities and a lot of waterbodies, most of the area is less susceptible to agricultural drought. Inadequate soil conditions, such as insufficient drainage or a deficiency of vital nutrients, further impede agricultural success. The soil type of Iowa is favorable to agricultural production. So, a few of the areas are vulnerable to these factors. In addition, areas with low population density have a low vulnerability to drought, except for main cities and populated areas. Additionally, environmental factors, such as extreme weather events and unfavorable climate conditions, contribute to the overall vulnerability.

Figure 5 (a-d) shows the fuzzy standardized maps of meteorological factors (T_{max}, PET, P, and SM) via color. Red spots show agricultural drought risk, while green areas indicate agricultural drought-resistant regions according to T_{max} (Fig. 4(a)), PET (Fig. 5(b)), precipitation (Fig. 5(c)), and soil moisture (Fig. 5(d)).

The variability of T_{max} is greatly influenced by various factors, including surface type, altitude, and other related factors. The cartographic depictions exhibit significant variation on an annual basis, not solely attributable to the characteristics mentioned above but also due to climatic variability. Similarly, it varies considerably in PET, and P. PET values depend on the air temperature and factors such as relative humidity and wind speed, which have quite chaotic properties (Baydaroğlu and Koçak, 2019). In addition to these factors, precipitation is affected by teleconnections (Villarini et al., 2013) and other synoptic scale movements (Elkhouly et al., 2023) in Iowa. Furthermore, the soil moisture spatial variability is complex due to the physical composition of the soil, in conjunction with the aforementioned meteorological factors (Wang et al., 2017).

3.2. Drought Vulnerability Mapping

Figure 6 illustrates the varying degrees of drought vulnerability observed in the study area from 2015 to 2021 based on the influence of several significant factors. The equal interval classification system divides drought vulnerability into five distinct classes, ranging from extremely low to extremely high. Observing that the spatial extent of drought vulnerability varies over the specified time period is essential. This data is presented in Table 3, which provides a percentage-based representation of the various drought vulnerability levels in different years. During the examined period, the majority of Iowa's land area exhibited low to moderate drought vulnerability. However, there were also high drought vulnerability instances, except in 2017 and 2021. These years (2017 and 2021) were recorded as when the drought was intensely felt in Iowa and Midwest.

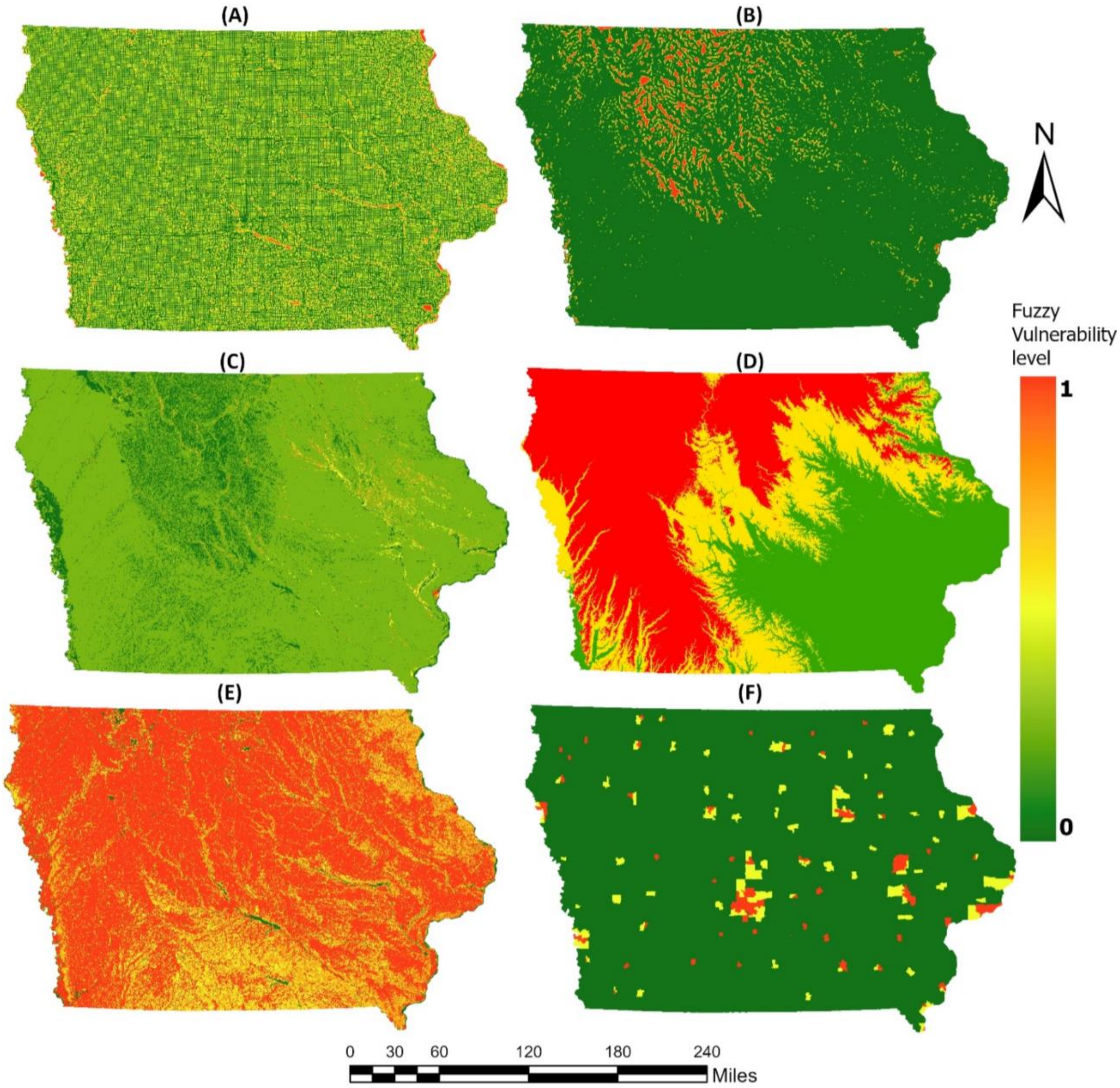

Figure 4. Fuzzy vulnerability mapping due to (a) distance to road, (b) distance to waterbody, (c) soil type, (d) elevation, (e) LULC, and (e) population density (2015-2021).

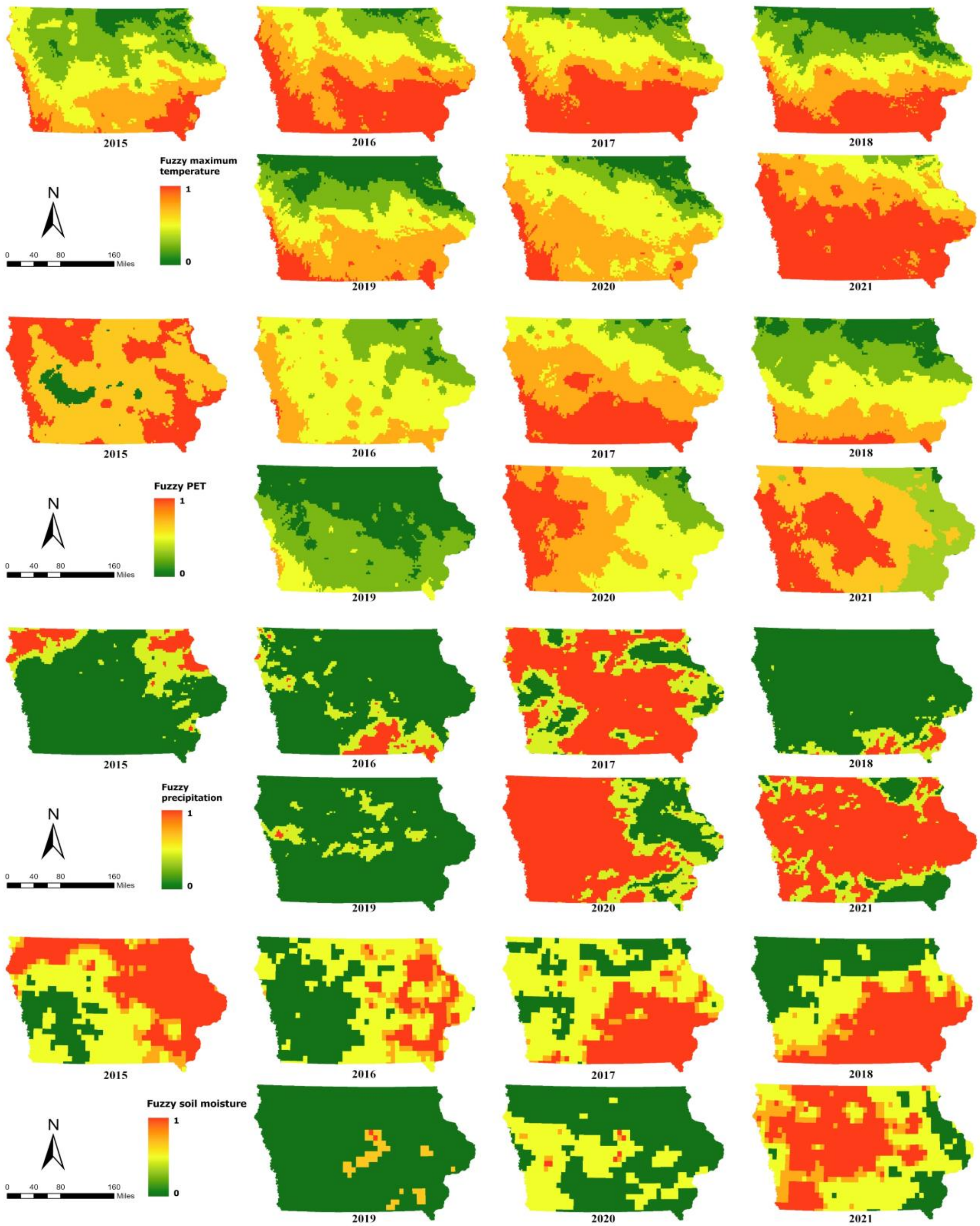

Figure 5. Fuzzy vulnerability mapping due to (a) maximum air temperature, (b) seasonal total PET, (c) seasonal total precipitation, and (d) soil moisture (2015-2021).

Table 3 calculated the total (moderate to very high) drought vulnerability levels as 22.7 and 22.5%, respectively. In 2021, approximately 0.32 percent of Iowa’s territory (equivalent to nearly 450 km^2) exhibited a very high level of drought vulnerability. In 2017, this level of vulnerability affected 0.1% of the state's population. Notably, despite both 2021 and 2017 exhibiting the maximum drought vulnerability levels, their spatial distributions differed considerably. In 2017, most of Iowa’s high and very high drought-vulnerability regions were in the state's center and southwest. In 2021, however, the state's middle north and northwest areas were more severely affected by drought. In addition, a discernible pattern of drought vulnerability arises when the entire period is considered. The level of drought vulnerability was at its lowest in 2015 and progressively increased until 2017. The spatial extent of vulnerability subsequently decreased until 2019, only to increase again in 2021. This cyclical pattern indicates fluctuating drought susceptibility over time. This analysis also illustrates the dynamic nature of drought vulnerability in the study area from 2015 to 2021. The classification and spatial distribution of vulnerability levels and observed patterns provide valuable insight into the impact and extent of drought in Iowa.

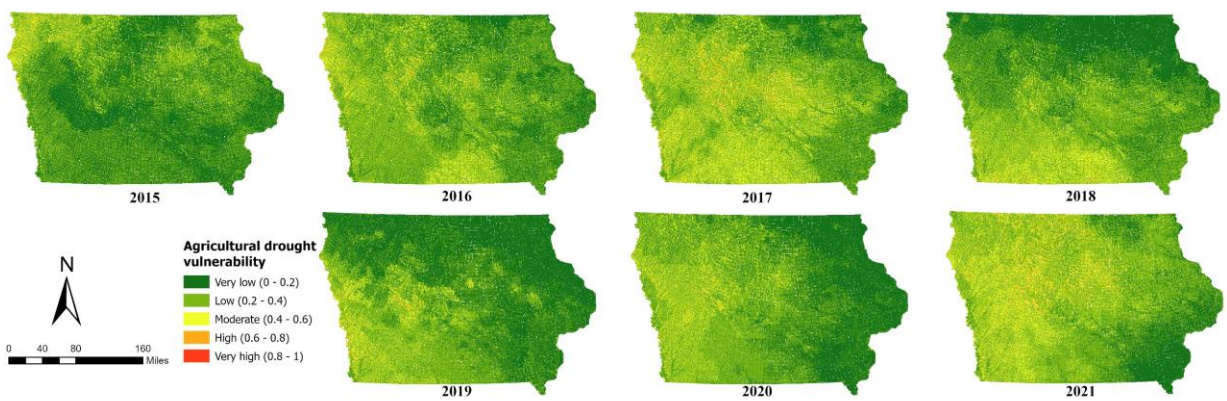

Figure 6. Drought vulnerability mapping of Iowa for the 2015–2021 period.

Table 3. Distribution of Drought Hazard Severity Levels by Percentage Area (2015-2021).

			Drought Vulnerability Level		
Year	**Very low**	**Low**	**Moderate**	**High**	**Very high**
2021	21.09	56.39	19.32	2.88	0.32
2020	33.84	48.80	15.29	2.00	0.06
2019	53.46	39.26	6.60	0.66	0.02
2018	43.39	46.25	9.91	0.44	0.01
2017	21.73	55.60	20.18	2.40	0.10
2016	30.79	57.71	10.79	0.69	0.01
2015	50.86	43.71	4.99	0.44	0.01

3.3. Drought Exposure Mapping

Figure 7 represents the spatial distribution of drought-vulnerable individuals, infrastructure, and natural resources within the study area. According to the analysis, approximately 78.4% (113,420.65 km^2) of the studied area is susceptible to moderate drought. Notably, areas characterized by a high population density and extensive development have a high prevalence of exposure to extremely severe drought. These vulnerable areas are dispersed throughout the state, indicating a far-reaching impact on various locations.

Upon closer inspection, it becomes clear that the state's middle and eastern regions confront elevated levels of drought exposure, including high and very high categories. This preponderance of vulnerability suggests that individuals, infrastructure, and environmental resources in these regions are exposed to increasing risk. Figure 8 also depicts the spatial distribution of drought vulnerability, an indispensable instrument for identifying and comprehending the regions within the study area most susceptible to drought-related risks. It emphasizes the imperative need for targeted interventions to mitigate the potential effects on communities, infrastructure, and essential resources by highlighting areas with high population density and extensive development.

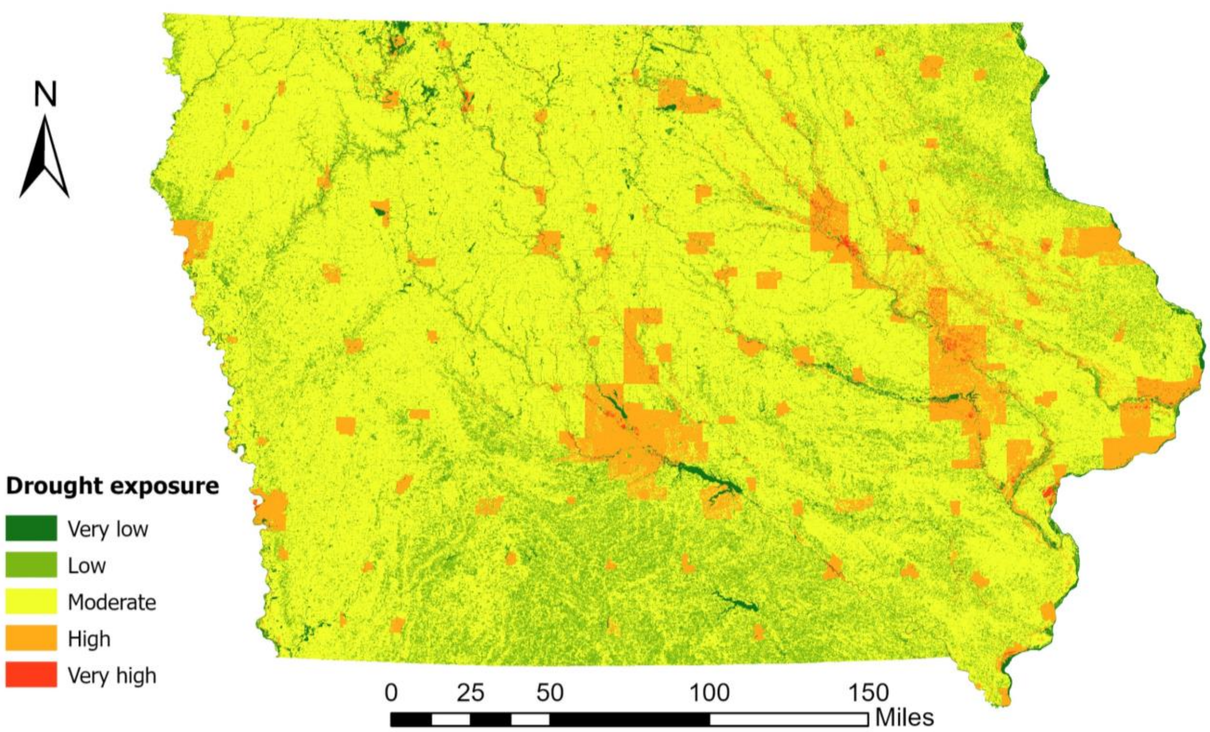

Figure 7. Drought exposure map of Iowa during the 2015-2021 period.

3.4. Drought Risk Mapping

The spatial distribution and severity levels of drought risk in the study area are depicted in Figure 9. In 2018, a "very high" level of drought risk (5.4%) was recorded, with nearly 16% of the land classified as being at "high" risk. Although most of the region experienced minimal risk, a sizable portion faces moderate to extremely high risk. In 2018, Iowa's southern and west-south regions exhibited a greater risk of drought. In 2021, the area at a "very high" risk of drought decreased to 4.5% of the study area, but the spatial distribution of drought was different than in 2018. Mid-Iowa and the western portion of the state exhibited increased high and extremely high drought threats. In 2019, moderate to "very high" drought risk affected approximately 36.0% of the study area, primarily in the state's western portion.

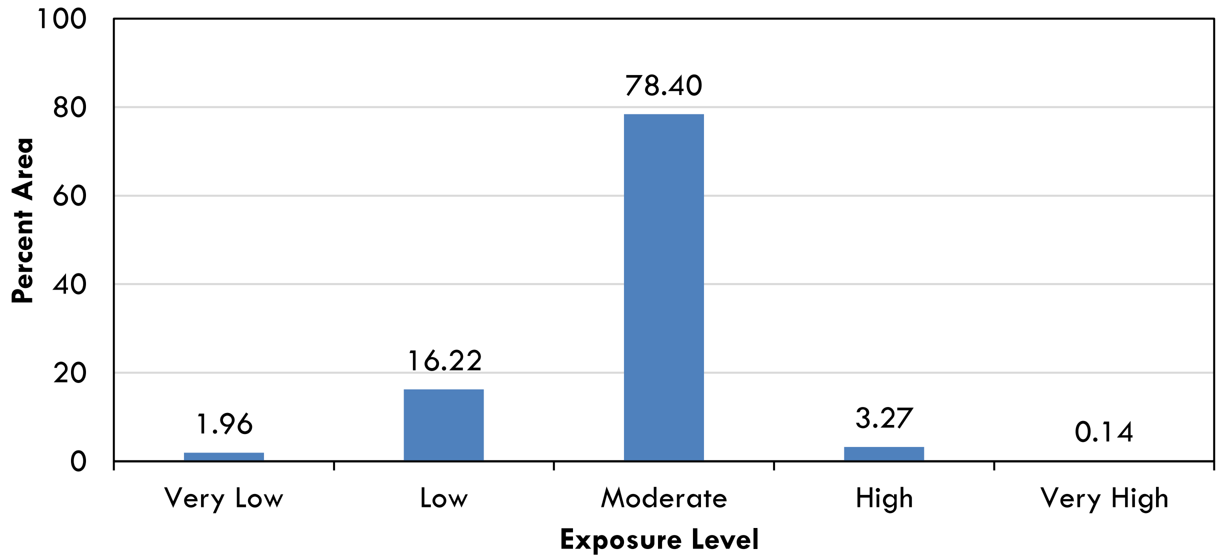

Figure 8. Agricultural drought exposure by area (%).

In contrast, regions with very low to moderate drought risk were primarily concentrated in Iowa's central and eastern regions and portions of the state's northeastern region. Given the fluctuating drought conditions in the region, crop yields are likely to be impacted from season to season (Figure 10). Further research is needed to investigate the level of drought's impact on crop production at the study site.

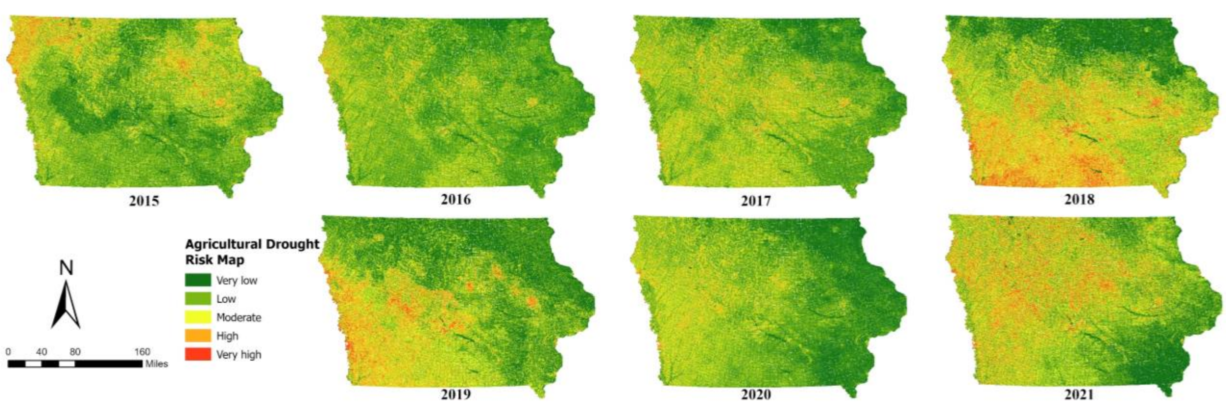

Figure 9. Agricultural drought risk map during the 2015-2021 period.

Table 4. Agricultural drought risk severity by the class during 2015-2021.

Year	Very low	Low	Moderate	High	Very high
2015	16.20	60.38	13.42	9.35	0.66
2016	28.88	44.14	18.36	6.73	1.89
2017	31.46	40.41	21.35	6.01	0.77
2018	22.42	28.59	27.63	15.97	5.39
2019	29.08	35.62	22.20	10.83	2.28
2020	42.67	36.45	16.76	3.83	0.30
2021	20.31	36.61	25.93	12.68	4.46

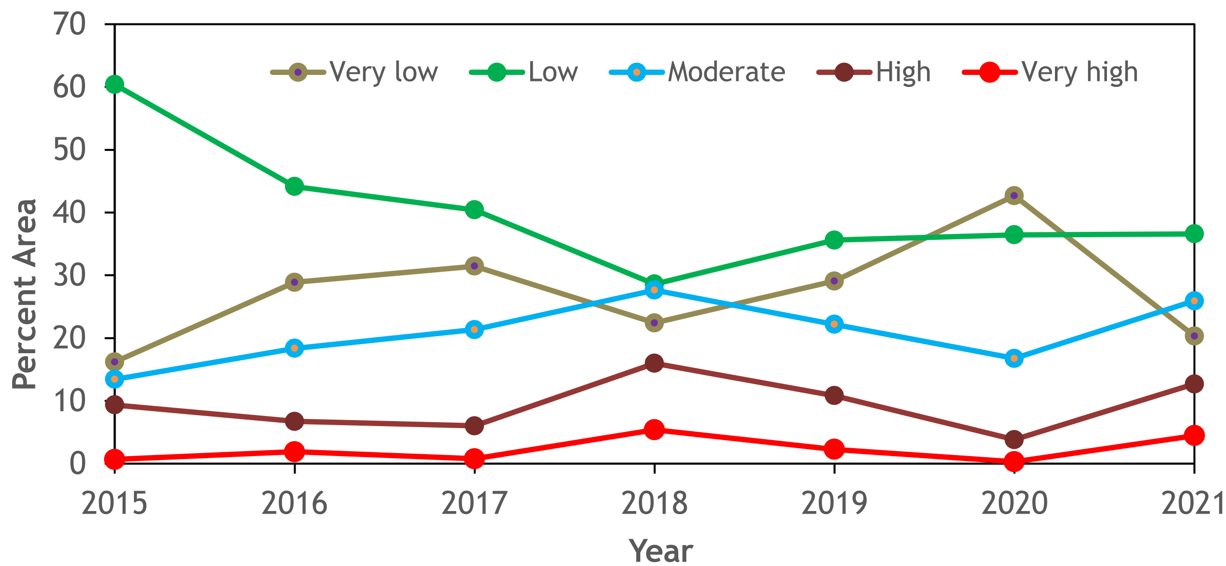

Figure 10. Percentage of the area under different risk levels of the study area.

3.5. Accuracy Assessment for Drought Risk Mapping

Accuracy assessment is a crucial step in evaluating the reliability and usefulness of any thematic mapping product (Foody, 2002). One commonly used technique for assessing the accuracy of categorical maps is the kappa coefficient, a statistical measure of agreement between the observed and expected classifications, accounting for the possibility of random agreement (Stehman, 1997). In this case, the kappa coefficient technique was used to assess the accuracy of your agricultural drought vulnerability mapping. This involved comparing the results of the agricultural drought vulnerability mapping with a ground-truth dataset that represents the actual drought occurrences in your study area. The SM data may be used to validate the agricultural drought vulnerability map because it is a crucial indicator of agricultural droughts (Kafy et al., 2023). Several studies (Hoque et al., 2021) mentioned SM data as a validation indicator for agricultural drought vulnerability. So, the SM data for 2021 was tested with 2021's vulnerability map here.

The Kappa coefficient technique helps evaluate the agreement between the mapped drought vulnerability classes and the actual drought occurrences (Núnez et al., 2011; Senapati and Das, 2022). The technique involves calculating the user accuracy, producer accuracy, overall accuracy, and kappa coefficient value. User accuracy measures the proportion of correctly classified pixels for each class. In contrast, producer accuracy measures the ratio of correctly classified pixels out of all the pixels predicted for each category (Ebrahimy et al., 2021). Overall accuracy measures the proportion of correctly classified pixels for all classes combined. The kappa coefficient value is a more robust measure of accuracy than overall accuracy. It accounts for the possibility of chance agreement between the mapped classes and the actual classes. A kappa coefficient value of 1 indicates perfect agreement between the observed and expected classifications, while 0 indicates no agreement beyond what would be expected by chance (Ebrahimy et al., 2021).

This study showed high user and producer accuracy for most classes, indicating that the mapping accurately classified pixels into their respective drought vulnerability classes. The overall accuracy was 81%, meaning that 81% of the mapped pixels were correctly classified. The Kappa coefficient value 0.75 indicates substantial agreement between the observed and expected classifications. This suggests that the mapping is robust and reliable and can be used to inform drought mitigation and management strategies.

Table 5. Validation of agricultural drought vulnerability map using Kappa-coefficient.

Accuracy Assessment								
Drought Level	Very Low	Low	Moderate	High	Very High	Row Total	User Accuracy	Kappa
Very low	18	3	4	2	0	27	0.43	0.00
Low	2	44	6	3	0	55	0.80	0.00
Moderate	1	2	35	9	3	50	0.70	0.00
High	0	0	3	50	1	54	0.93	0.00
Very high	0	0	0	5	35	40	0.88	0.00
Column Total	21	49	48	69	39	226	0.00	0.00
Producer Accuracy	0.86	0.90	0.73	0.72	0.90	0.00	0.31	0.00
Kappa	0	0	0	0	0	0	0	**0.75**

4. Conclusion

Due to their spatiotemporal variability, determining the impact of meteorological factors on agricultural drought is a complex undertaking. Moreover, agricultural drought is a multifaceted phenomenon that cannot be comprehensively elucidated solely by meteorological parameters. This study incorporated meteorological factors and physical and social indicators from a particular perspective.

A thorough drought risk mapping approach incorporating all risk components is particularly effective for reducing the difficulties of production losses, ecology, and overall economic impact. Many studies have been conducted utilizing various geospatial methodologies to evaluate the condition of agricultural drought in Iowa. Nevertheless, this research has concentrated on multicriteria risk factors, including meteorological factors, soil type and properties, and social properties. This research presents a comprehensive analysis of Iowa's drought vulnerability in the study area from 2015 to 2021. The study used an equal interval classification method to categorize drought vulnerability into five classes.

The results indicate that most of Iowa's land area experienced low to moderate drought vulnerability during the examined period, with occasional instances of extremely high vulnerability in 2017 and 2021. Almost 85% of the land in Iowa is exploited for farming, making it a crucial business. Because of this, the state is quite susceptible to agricultural drought, which may significantly affect crop output, animal production, and the economy as a whole. According to future projection studies (Jin et al., 2017; Leng and Hall, 2019) conducted on the study area, it has been identified that it is likely to experience crucial agricultural drought-induced damage concerning the production of maize and soybean crops. This study may contribute significantly to the endeavors of decision-makers, farmers' associations, and local administrations in addressing the potential environmental and socioeconomic consequences of agricultural drought.

The analysis reveals a pattern of fluctuating drought vulnerability over time, with vulnerability levels increasing until 2017, decreasing until 2019, and then increasing again in 2021. Research findings indicate that around 82% of the geographical area of Iowa, of which 85% is utilized for agricultural purposes, exhibits susceptibility to drought conditions. Furthermore, the research underscores the spatial arrangement of regions prone to drought, accentuating the greater vulnerability of areas with dense populations and significant development. The regions in the state's middle and eastern parts have been identified as being subjected to heightened levels of susceptibility to drought. The results emphasize the fluid characteristic of susceptibility to drought and furnish valuable discernments into the ramifications and scope of drought in Iowa.

The proposed approach can assist in determining which parts of Iowa are most at risk from drought and help prioritize efforts to take drought mitigation measures. The drought risk assessment approach might be improved by including mitigation capabilities in the final risk calculation. It is important to remember that gathering high-quality datasets can be challenging, and higher-resolution datasets can be needed for more precise outcomes. Overall, the integrated fuzzy logic approach can produce results that are suitable for mapping Iowa's agricultural drought, creating drought mitigation plans, and preserving sustainable development. Future studies may deal with data limitations and create optimized data standards and formats (Demir and Szczepanek, 2017) to boost validation procedures and output accuracy. Further research is encouraged to explore the specific impact of drought on crop production in the state.

References

Aitkenhead, I., Kuleshov, Y., Watkins, A. B., Bhardwaj, J., & Asghari, A. (2021). Assessing agricultural drought management strategies in the Northern Murray–Darling Basin. *Natural Hazards*, *109*(2), 1425-1455. https://doi.org/10.1007/s11069-021-04884-6

American Heritage Dictionary Entry: Iowa. (2023). https://www.ahdictionary.com/word/search.html?q=Iowa

Alabbad, Y., Yildirim, E., & Demir, I. (2022). Flood mitigation data analytics and decision support framework: Iowa Middle Cedar Watershed case study. Science of The Total Environment, 814, 152768.

Bannayan, M., Sanjani, S., Alizadeh, A., Lotfabadi, S. S., & Mohamadian, A. (2010). Association between climate indices, aridity index, and rainfed crop yield in northeast of Iran. *Field Crops Research*, *118*(2), 105–114. https://doi.org/10.1016/j.fcr.2010.04.011

Baydaroğlu, Ö., & Koçak, K. (2019). Spatiotemporal analysis of wind speed via the Bayesian maximum entropy approach. *Environmental Earth Sciences*, *78*(1), 17. https://doi.org/10.1007/s12665-018-8024-z

Baydaroğlu Yeşilköy, Ö., Koçak, K., & Şaylan, L. (2020). Prediction of commonly used drought indices using support vector regression powered by chaotic approach. *Italian Journal of Agrometeorology*, (2), 65-76. https://doi.org/10.13128/ijam-970

Beaudoing, Hiroko, M. Rodell, A. Getirana, and B. Li, NASA/GSFC/HSL (2021), Groundwater and Soil Moisture Conditions from GRACE and GRACE-FO Data Assimilation L4 7-days 0.125 x 0.125 degree U.S. V4.0, Greenbelt, MD, USA, Goddard Earth Sciences Data and Information Services Center (GES DISC), (Last Accessed on March 30, 2023) https://doi.org/10.5067/UH653SEZR9VQ

Beck, M.B., Jiang, F., Shi, F., Walker, R.V., Osidele, O.O., Lin, Z., Demir, I. and Hall, J.W., (2010, March). Re-engineering cities as forces for good in the environment. In Proceedings of the Institution of Civil Engineers-Engineering Sustainability (Vol. 163, No. 1, pp. 31-46). Thomas Telford Ltd.

Beck, H. E., Zimmermann, N. E., McVicar, T. R., Vergopolan, N., Berg, A., & Wood, E. F. (2018). Present and future Köppen-Geiger climate classification maps at 1-km resolution. *Scientific data*, *5*(1), 1-12. https://doi.org/10.1038/sdata.2018.214

Benami, E., Jin, Z., Carter, M. R., Ghosh, A., Hijmans, R. J., Hobbs, A., ... & Lobell, D. B. (2021). Uniting remote sensing, crop modelling and economics for agricultural risk management. *Nature Reviews Earth & Environment*, *2*(2), 140-159. https://doi.org/10.1038/s43017-020-00122-y

Bodmer, R., Mayor, P., Antunez, M., Chota, K., Fang, T., Puertas, P., ... & Docherty, E. (2018). Major shifts in Amazon wildlife populations from recent intensification of floods and drought. *Conservation Biology*, *32*(2), 333-344. https://doi.org/10.1111/cobi.12993

Burke, M., & Emerick, K. (2016). Adaptation to climate change: Evidence from U.S. agriculture. *American Economic Journal: Economic Policy*, *8*(3), 106–140. https://doi.org/10.1257/pol.20130025

Cos, J., Doblas-Reyes, F., Jury, M., Marcos, R., Bretonnière, P. A., & Samsó, M. (2022). The Mediterranean climate change hotspot in the CMIP5 and CMIP6 projections. *Earth System Dynamics*, *13*(1), 321-340. https://doi.org/10.5194/esd-13-321-2022

Cikmaz, B. A., Yildirim, E., & Demir, I. (2023). Flood susceptibility mapping using fuzzy analytical hierarchy process for cedar rapids, Iowa. International Journal of River Basin Management, 1-13.

Dahal, P., Shrestha, N. S., Shrestha, M. L., Krakauer, N. Y., Panthi, J., Pradhanang, S. M., Jha, A., & Lakhankar, T. (2016). Drought risk assessment in central Nepal: temporal and spatial analysis. *Natural Hazards*, *80*, 1913–1932. https://doi.org/10.1007/s11069-015-2055-5

Dai, A. (2011). Drought under global warming: a review. *Wiley Interdisciplinary Reviews: Climate Change*, *2*(1), 45–65. https://doi.org/10.1002/wcc.81

Dayal, K., Deo, R., & Apan, A. A. (2017). Drought modelling based on artificial intelligence and neural network algorithms: a case study in Queensland, Australia. *Climate Change Adaptation in Pacific Countries: Fostering Resilience and Improving the Quality of Life*, 177–198. https://doi.org/10.1007/978-3-319-50094-2_11

Demir, I., Conover, H., Krajewski, W.F., Seo, B.C., Goska, R., He, Y., McEniry, M.F., Graves, S.J. and Petersen, W., (2015). Data-enabled field experiment planning, management, and research using cyberinfrastructure. Journal of Hydrometeorology, 16(3), pp.1155-1170.

Demir, I., Jiang, F., Walker, R. V., Parker, A. K., & Beck, M. B. (2009, October). Information systems and social legitimacy scientific visualization of water quality. In 2009 IEEE International Conference on Systems, Man and Cybernetics (pp. 1067-1072). IEEE.

Demir, I., & Szczepanek, R. (2017). Optimization of river network representation data models for web-based systems. Earth and Space Science, 4(6), 336-347.

Ebrahimy, H., Mirbagheri, B., Matkan, A. A., & Azadbakht, M. (2021). Per-pixel land cover accuracy prediction: A random forest-based method with limited reference sample data. ISPRS Journal of Photogrammetry and Remote Sensing, 172, 17–27. https://doi.org/10.1016/j.isprsjprs.2020.11.024

Ekrami, M., Marj, A. F., Barkhordari, J., & Dashtakian, K. (2016). Drought vulnerability mapping using AHP method in arid and semiarid areas: a case study for Taft Township, Yazd Province, Iran. *Environmental Earth Sciences*, *75*, 1-13. https://doi.org/10.1007/s12665-016-5822-z

Elkhouly, M., Zick, S. E., & Ferreira, M. A. (2023). Long term temporal trends in synoptic-scale weather conditions favoring significant tornado occurrence over the central United States. *PLoS one*, *18*(2), e0281312. https://doi.org/10.1371/journal.pone.0281312

EM-DAT (2023a) https://public.emdat.be/ (Last Accessed on March 20, 2023)

EM-DAT (2023b) 2022 Disasters in numbers. https://cred.be/sites/default/files/2022_EMDAT_report.pdf

FEMA. (1995). United States. Federal Emergency Management Agency. *Federal Response Plan for Drought. Washington, D.C.*

Foody, G. M. (2002). Status of land cover classification accuracy assessment. Remote Sensing of Environment, 80(1), 185–201. DOI: https://doi.org/10.1016/S0034-4257(01)00295-4

García-León, D., Standardi, G., & Staccione, A. (2021). An integrated approach for the estimation of agricultural drought costs. *Land Use Policy*, *100*, 104923. https://doi.org/10.1016/j.landusepol.2020.104923

Guo, H., Chen, J., & Pan, C. (2021). Assessment on agricultural drought vulnerability and spatial heterogeneity study in China. *International Journal of Environmental Research and Public Health*, *18*(9), 4449. https://doi.org/10.3390/ijerph18094449

Hatfield, J. L., & Prueger, J. H. (2015). Temperature extremes: Effect on plant growth and development. *Weather and Climate Extremes*, *10*, 4–10. https://doi.org/10.1016/j.wace.2015.08.001

Hobbins, M. T., Wood, A., McEvoy, D. J., Huntington, J. L., Morton, C., Anderson, M., & Hain, C. (2016). The evaporative demand drought index. Part I: Linking drought evolution to variations in evaporative demand. *Journal of Hydrometeorology*, *17*(6), 1745-1761. https://doi.org/10.1175/JHM-D-15-0121.1

Hoque, M. A. A., Pradhan, B., Ahmed, N., & Sohel, M. S. I. (2021). Agricultural drought risk assessment of Northern New South Wales, Australia using geospatial techniques. Science of the Total Environment, 756, 143600. https://doi.org/10.1016/j.scitotenv.2020.143600

Iowa Farm Facts. (2023). Living History Farms | Learning-Fields. https://www.lhf.org/learning-fields/crops/iowa-farm-facts/

Iowa Quick Facts — State Data Center. (2023). https://web.archive.org/web/20210501075540/https://www.iowadatacenter.org/quickfacts

Iowa DNR, (2023). Iowa Drought Plan. Retrieved from: https://www.iowadnr.gov/Portals/idnr/uploads/files/2023-iowa-drought-plan.pdf

IV, W. T., & Nathan, T. R. (2022). El Niño–Southern Oscillation and the Transatlantic Slave Trade. *Weather, Climate, and Society*, *14*(1), 257–271. https://doi.org/10.1175/WCAS-D-21-0036.1

Islam, S. S., Islam, K. A., & Mullick, M. R. A. (2022). Drought hot spot analysis using local indicators of spatial autocorrelation: An experience from Bangladesh. *Environmental Challenges*, *6*, 100410. https://doi.org/10.1016/j.envc.2021.100410

Jain, V. K., Pandey, R. P., & Jain, M. K. (2015). Spatio-temporal assessment of vulnerability to drought. *Natural Hazards*, *76*, 443–469. https://doi.org/10.1007/s11069-014-1502-z

Jin, Z., Zhuang, Q., Wang, J., Archontoulis, S. V., Zobel, Z., & Kotamarthi, V. R. (2017). The combined and separate impacts of climate extremes on the current and future U.S. rainfed maize and soybean production under elevated CO2. *Global change biology*, *23*(7), 2687-2704. https://doi.org/10.1111/gcb.13617

Kafy, A. A., Bakshi, A., Saha, M., Al Faisal, A., Almulhim, A. I., Rahaman, Z. A., & Mohammad, P. (2023). Assessment and prediction of index based agricultural drought vulnerability using machine learning algorithms. *Science of The Total Environment*, 161394. https://doi.org/10.1016/j.scitotenv.2023.161394

Kahraman, C. (2008). Multicriteria decision making methods and fuzzy sets. *Fuzzy Multicriteria Decision Making: Theory and Applications with Recent Developments*, 1–18. https://doi.org/10.1007/978-0-387-76813-7_1

Kimm, H., Guan, K., Gentine, P., Wu, J., Bernacchi, C. J., Sulman, B. N., ... & Lin, C. (2020). Redefining droughts for the US Corn Belt: The dominant role of atmospheric vapor pressure deficit over soil moisture in regulating stomatal behavior of Maize and Soybean. *Agricultural and Forest Meteorology*, *287*, 107930. https://doi.org/10.1016/j.rse.2021.112833

Kumar, K. A., Reddy, G. O., Masilamani, P., Turkar, S. Y., & Sandeep, P. (2021). Integrated drought monitoring index: A tool to monitor agricultural drought by using time-series datasets of space-based earth observation satellites. *Advances in Space Research*, *67*(1), 298-315. https://doi.org/10.1016/j.asr.2020.10.003

Kumar, S. S., Arivazhagan, S., & Rangarajan, N. (2013). Remote sensing and GIS applications in Environmental Sciences--A review. J. Environ. Nanotechnol, 2(2), 92–101.https://doi.org/10.13074/jent.2013.06.132025

Kundu, A., Dutta, D., Patel, N. R., Denis, D. M., & Chattoraj, K. K. (2021). Evaluation of socioeconomic drought risk over bundelkhand region of India using analytic hierarchy process (AHP) and geospatial techniques. *Journal of the Indian Society of Remote Sensing*, *49*, 1365-1377. https://doi.org/10.1007/s12524-021-01306-9

Leeper, R. D., Bilotta, R., Petersen, B., Stiles, C. J., Heim, R., Fuchs, B., ... & Ansari, S. (2022). Characterizing U.S. drought over the past 20 years using the U.S. drought monitor. *International Journal of Climatology*, *42*(12), 6616-6630. https://doi.org/10.1002/joc.7653

Leng, G., & Hall, J. (2019). Crop yield sensitivity of global major agricultural countries to droughts and the projected changes in the future. *Science of the Total Environment*, *654*, 811-821. https://doi.org/10.1016/j.scitotenv.2018.10.434

Li, Z., & Demir, I. (2023). U-net-based semantic classification for flood extent extraction using SAR imagery and GEE platform: A case study for 2019 central US flooding. Science of The Total Environment, 869, 161757.

Littell, J. S., Peterson, D. L., Riley, K. L., Liu, Y., & Luce, C. H. (2016). A review of the relationships between drought and forest fire in the United States. *Global Change Biology*, *22*(7), 2353–2369. DOI: https://doi.org/10.1111/gcb.13275

Lobell, D. B., Schlenker, W., & Costa-Roberts, J. (2011). Climate trends and global crop production since 1980. *Science*, *333*(6042), 616–620. DOI: https://doi.org/10.1126/science.1204531

Madakumbura, G. D., Kim, H., Utsumi, N., Shiogama, H., Fischer, E. M., Seland, Ø., ... & Oki, T. (2019). Event-to-event intensification of the hydrologic cycle from 1.5°C to a 2°C warmer world. *Scientific Reports*, *9*(1), 1-7. https://doi.org/10.1038/s41598-019-39936-2

Mallya, G., Zhao, L., Song, X. C., Niyogi, D., & Govindaraju, R. S. (2013). 2012 Midwest drought in the United States. *Journal of Hydrologic Engineering*, *18*(7), 737-745. https://doi.org/10.1061/(ASCE)HE.1943-5584.0000786

Mani, J.K., Varghese, A.O. (2018). Remote Sensing and GIS in Agriculture and Forest Resource Monitoring. In: Reddy, G., Singh, S. (eds) Geospatial Technologies in Land Resources Mapping, Monitoring and Management. Geotechnologies and the Environment, vol 21. Springer, Cham. https://doi.org/10.1007/978-3-319-78711-4_19

Menne, M. J., Durre, I., Korzeniewski, B., McNeal, S., Thomas, K., Yin, X., Anthony, S., Ray, R., Vose, R. S., Gleason, B. E., & others. (2012). *Global historical climatology network-daily (Version 3.24). NOAA National Climatic Data Center*. https://doi.org/10.1175/JTECH-D-11-00103.1

Mishra, A. K., & Singh, V. P. (2011). Drought modeling--A review. *Journal of Hydrology*, *403*(1–2), 157–175. https://doi.org/10.1016/j.jhydrol.2011.03.049

Mokarram, M., Pourghasemi, H. R., Hu, M., & Zhang, H. (2021). Determining and forecasting drought susceptibility in southwestern Iran using multicriteria decision-making (MCDM) coupled with CA-Markov model. *Science of the Total Environment*, *781*, 146703. https://doi.org/10.1016/j.scitotenv.2021.146703

Mukherjee, S., Mishra, A., & Trenberth, K. E. (2018). Climate change and drought: a perspective on drought indices. Current climate change reports, 4, 145-163. DOI: https://doi.org/10.1007/s40641-018-0098-x

Mullick, M. R. A., Tanim, A. H., & Islam, S. M. S. (2019). Coastal vulnerability analysis of Bangladesh coast using fuzzy logic based geospatial techniques. *Ocean and Coastal Management*, *174*, 154–169. https://doi.org/10.1016/j.ocecoaman.2019.03.010

Muste, M., Lyn, D. A., Admiraal, D., Ettema, R., Nikora, V., & García, M. H. (Eds.). (2017). Experimental hydraulics: Methods, instrumentation, data processing and management: Volume I: Fundamentals and methods. CRC Press.

Narasimhan, B., & Srinivasan, R. (2005). Development and evaluation of Soil Moisture Deficit Index (SMDI) and Evapotranspiration Deficit Index (ETDI) for agricultural drought monitoring. *Agricultural and forest meteorology*, *133*(1-4), 69-88. https://doi.org/10.1016/j.agrformet.2005.07.012

Nikolova, N., Zlateva, P., & Todorov, L. (2021). Fuzzy Logic Approach to Complex Assessment of Drought Vulnerability. *IFIP Advances in Information and Communication Technology*, *622*, 298–314. https://doi.org/10.1007/978-3-030-81469-4_24/TABLES/7

NOAA. (2023). *Iowa | Drought.gov*. https://www.drought.gov/states/iowa (Last Accessed on March 20, 2023)

Núnez, J. H., Verbist, K., Wallis, J. R., Schaefer, M. G., Morales, L., & Cornelis, W. M. (2011). Regional frequency analysis for mapping drought events in north-central Chile. *Journal of Hydrology*, *405*(3–4), 352–366. https://doi.org/10.1016/j.jhydrol.2011.05.035

O'Neill, B. C., Carter, T. R., Ebi, K., Harrison, P. A., Kemp-Benedict, E., Kok, K., Kriegler, E., Preston, B. L., Riahi, K., Sillmann, J., & others. (2020). Achievements and needs for the climate change scenario framework. *Nature Climate Change*, *10*(12), 1074–1084. https://doi.org/10.1038/s41558-020-00952-0

Ortega-Gaucin, D., Ceballos-Tavares, J. A., Ordoñez Sánchez, A., & Castellano-Bahena, H. V. (2021). Agricultural drought risk assessment: A spatial analysis of hazard, exposure, and vulnerability in Zacatecas, Mexico. *Water*, *13*(10), 1431. https://doi.org/10.3390/w13101431

Pedro-Monzonís, M., Solera, A., Ferrer, J., Estrela, T., & Paredes-Arquiola, J. (2015). A review of water scarcity and drought indexes in water resources planning and management. *Journal of Hydrology*, *527*, 482-493. https://doi.org/10.1016/j.jhydrol.2015.05.003

Pesti, G., Shrestha, B. P., Duckstein, L., & Bogárdi, I. (1996). A fuzzy rule-based approach to drought assessment. *Water Resources Research*, *32*(6), 1741-1747. https://doi.org/10.1029/96WR00271

Pramanik, D., Mondal, S. C., & Haldar, A. (2020). A framework for managing uncertainty in information system project selection: An intelligent fuzzy approach. *International Journal of Management Science and Engineering Management*, *15*(1), 70–78. https://doi.org/10.1080/17509653.2019.1604191

Prior, J. C. (1991). *Landforms of Iowa*. University of Iowa Press.

Schumacher, D. L., Keune, J., Dirmeyer, P., & Miralles, D. G. (2022). Drought self-propagation in drylands due to land–atmosphere feedbacks. *Nature geoscience*, *15*(4), 262-268. https://doi.org/10.1038/s41561-022-00912-7

Senapati, U., Raha, S., Das, T. K., & Gayen, S. K. (2021). A composite assessment of agricultural drought susceptibility using analytic hierarchy process: Case study of western region of West Bengal. *Agriculture, Food and Nutrition Security: A Study of Availability and Sustainability in India*, 15-40. https://doi.org/10.1007/978-3-030-69333-6_2

Senapati, U., & Das, T. K. (2022). Geospatial assessment of agricultural drought vulnerability using integrated three-dimensional model in the Upper Dwarakeshwar River Basin In West Bengal, India. *Environmental Science and Pollution Research*, 1-28. https://doi.org/10.1007/s11356-022-23663-9

Sepulcre-Canto, G., Horion, S., Singleton, A., Carrao, H., & Vogt, J. (2012). Development of a Combined Drought Indicator to detect agricultural drought in Europe. *Natural Hazards and Earth System Sciences*, *12*(11), 3519–3531. https://doi.org/10.5194/nhess-12-3519-2012

Sivakumar, V. L., Krishnappa, R. R., & Nallanathel, M. (2021). Drought vulnerability assessment and mapping using Multicriteria decision making (MCDM) and application of Analytic Hierarchy process (AHP) for Namakkal District, Tamilnadu, India. *Materials Today: Proceedings*, *43*, 1592-1599. https://doi.org/10.1016/j.matpr.2020.09.657

Seager, R., Naik, N., & Vogel, L. (2012). Does global warming cause intensified interannual hydroclimate variability?. *Journal of Climate*, *25*(9), 3355-3372. https://doi.org/10.1175/JCLI-D-11-00363.1

Sermet, Y., & Demir, I. (2023). Camera-based intelligent stream stage sensing for decentralized environmental monitoring. Journal of hydroinformatics, 25(2), 163-173.

Sit, M., Langel, R. J., Thompson, D., Cwiertny, D. M., & Demir, I. (2021). Web-based data analytics framework for well forecasting and groundwater quality. Science of the Total Environment, 761, 144121.

Sit, M., Demiray, B., & Demir, I. (2021). Short-term hourly streamflow prediction with graph convolutional GRU networks. arXiv preprint arXiv:2107.07039.

Stehman, S. V. (1997). Selecting and interpreting measures of thematic classification accuracy. Remote Sensing of Environment, 62(1), 77–89. https://doi.org/10.1016/S0034-4257(97)00083-7

Stephan, R., Terzi, S., Erfurt, M., Cocuccioni, S., Stahl, K., & Zebisch, M. (2022). Assessing agriculture's vulnerability to drought in European pre-Alpine regions. EGUsphere, 1-28. https://doi.org/10.5194/egusphere-2022-744

Steven Manson, J. S. (2021). *IPUMS national historical geographic information system: version*

15.0. http://doi.org/10.18128/D050.V15.0
Spinoni, J., Barbosa, P., Bucchignani, E., Cassano, J., Cavazos, T., Christensen, J. H., ... & Dosio, A. (2020). Future global meteorological drought hot spots: a study based on CORDEX data. *Journal of Climate*, *33*(9), 3635-3661. https://doi.org/10.1175/JCLI-D-19-0084.1
Tabari, H. (2020) Climate change impact on flood and extreme precipitation increases with water availability. *Sci Rep* 10, 13768. https://doi.org/10.1038/s41598-020-70816-2
Thomas, D. S., Wilhelmi, O. V., Finnessey, T. N., & Deheza, V. (2013). A comprehensive framework for tourism and recreation drought vulnerability reduction. *Environmental Research Letters*, *8*(4), 044004. https://doi.org/10.1088/1748-9326/8/4/044004
Tian, L., Yuan, S., & Quiring, S. M. (2018). Evaluation of six indices for monitoring agricultural drought in the south-central United States. *Agricultural and forest meteorology*, *249*, 107-119. https://doi.org/10.1016/j.agrformet.2017.11.024
USDA. (2016). *Natural Resources Conservation Service*. U.S. DEPARTMENT OF AGRICULTURE. https://www.nrcs.usda.gov/
USDA, (2021a). Emergency Relief Program (ERP) Drought Eligible Counties in 2021. Retrieved from: https://www.fsa.usda.gov/news-room/news-releases/2022/usda-to-provide-approximately-6-billion-to-commodity-and-specialty-crop-producers-impacted-by-2020-and-2021-natural-disasters
USDA. (2021b). *USDA - National Agricultural Statistics Service - Iowa - Crop Reports*. 2021. https://www.nass.usda.gov/Statistics_by_State/Iowa/Publications/Crop_Report/
Vicente-Serrano, S. M., Beguería, S., & López-Moreno, J. I. (2010). A multiscalar drought index sensitive to global warming: the standardized precipitation evapotranspiration index. *Journal of climate*, *23*(7), 1696-1718. https://doi.org/10.1175/2009JCLI2909.1
Villarini, G., Smith, J. A., Vitolo, R., & Stephenson, D. B. (2013). On the temporal clustering of U.S. floods and its relationship to climate teleconnection patterns. *International Journal of Climatology*, *33*(3), 629-640. https://doi.org/10.1002/joc.3458
Walthall, C. L., Hatfield, J., Backlund, P., Lengnick, L., Marshall, E., Walsh, M., Adkins, S., Aillery, M., Ainsworth, E. A., Ammann, C., & others. (2012). Climate change and agriculture in the United States: Effects and adaptation. USDA Technical Bulletin 1935. Washington, DC. *U.S. Department of Agriculture*.
Wang, Q., Wu, J., Lei, T., He, B., Wu, Z., Liu, M., ... & Liu, D. (2014). Temporal-spatial characteristics of severe drought events and their impact on agriculture on a global scale. *Quaternary International*, *349*, 10-21. https://doi.org/10.1016/j.quaint.2014.06.021
Wang, T., Franz, T. E., Li, R., You, J., Shulski, M. D., & Ray, C. (2017). Evaluating climate and soil effects on regional soil moisture spatial variability using EOF s. *Water Resources Research*, *53*(5), 4022-4035. https://doi.org/10.1002/2017WR020642
Wang, M., Liu, T., Ling, S., Sui, X., Yao, H., & Hou, X. (2019). Summary of agricultural drought monitoring by remote sensing at home and abroad. *IFIP Advances in Information and Communication Technology*, *546*, 13–20. https://doi.org/10.1007/978-3-030-06179-1_2/COVER

Wijitkosum, S., & Sriburi, T. (2019). Fuzzy AHP integrated with GIS analyses for drought risk assessment: A case study from upper Phetchaburi River basin, Thailand. *Water*, *11*(5), 939. https://doi.org/10.3390/w11050939

Wu, J., Geng, G., Zhou, H., Liu, J., Wang, Q., & Yang, J. (2017a). Global vulnerability to agricultural drought and its spatial characteristics. *Science China Earth Sciences, 60*, 910-920. https://doi.org/10.1007/s11430-016-9018-2

Wu, J., Lin, X., Wang, M., Peng, J., & Tu, Y. (2017b). Assessing agricultural drought vulnerability by a VSD Model: A case study in Yunnan Province, China. *Sustainability, 9*(6), 918. https://doi.org/10.3390/su9060918

Wu, H., Qian, H., Chen, J., & Huo, C. (2017c). Assessment of agricultural drought vulnerability in the Guanzhong Plain, China. *Water Resources Management*, *31*, 1557–1574. https://doi.org/10.1007/s11269-017-1594-9

Xu, H., Demir, I., Koylu, C., & Muste, M. (2019). A web-based geovisual analytics platform for identifying potential contributors to culvert sedimentation. *Science of the Total Environment*, 692, 806-817.

Yang, S. E., & Wu, B. F. (2010). Agricultural drought monitoring using web-serviced remote sensing data. *IC4E 2010 - 2010 International Conference on e-Education, e-Business, e-Management and e-Learning*, 532–535. https://doi.org/10.1109/IC4E.2010.61

Yeşilköy, S., & Şaylan, L. (2022). Spatial and temporal drought projections of northwestern Turkey. *Theoretical and Applied Climatology*, *149*(1-2), 1-14. https://doi.org/10.1007/s00704-022-04029-0

Yeşilköy, S., Baydaroğlu, Ö., & Demir, I. (2023). Is Snow Drought a Messenger for the Upcoming Severe Drought Period? A Case Study in the Upper Mississippi River Basin. *EarhArxiv*. https://doi.org/10.31223/X5S678

Yildirim, E., & Demir, I. (2022). Agricultural flood vulnerability assessment and risk quantification in Iowa. *Science of The Total Environment*, *826*, 154165. https://doi.org/10.1016/j.scitotenv.2022.154165

Yuan, X., Wang, Y., Ji, P., Wu, P., Sheffield, J., & Otkin, J. A. (2023). A global transition to flash droughts under climate change. *Science*, *380*, 187-191. https://doi.org/10.1126/science.abn6301

Zarei, A. R., Moghimi, M. M., & Koohi, E. (2021). Sensitivity assessment to the occurrence of different types of droughts using GIS and AHP techniques. *Water Resources Management, 35*, 3593-3615. https://doi.org/10.1007/s11269-021-02906-3

Zarei, A. R., & Mahmoudi, M. R. (2022). Assessing and predicting the vulnerability to agrometeorological drought using the fuzzy-AHP and second-order markov chain techniques. *Water Resources Management*, *36*(11), 4403-4424. https://doi.org/10.1007/s11269-022-03260-8

Zhao, H., & Li, N. (2016). Optimal siting of charging stations for electric vehicles based on fuzzy Delphi and hybrid multicriteria decision making approaches from an extended sustainability perspective. *Energies*, *9*(4), 270. https://doi.org/10.3390/en9040270

Zhou, W., Guan, K., Peng, B., Wang, Z., Fu, R., Li, B., ... & Chen, Z. (2021). A generic risk assessment framework to evaluate historical and future climate-induced risk for rainfed corn and soybean yield in the U.S. Midwest. *Weather and Climate Extremes*, *33*, 100369. https://doi.org/10.1016/j.wace.2021.100369

Zhou, R., Jin, J., Cui, Y., Ning, S., Bai, X., Zhang, L., ... & Tong, F. (2022). Agricultural drought vulnerability assessment and diagnosis based on entropy fuzzy pattern recognition and subtraction set pair potential. *Alexandria Engineering Journal*, *61*(1), 51-63. https://doi.org/10.1016/j.aej.2021.04.090